

## Modelling and optimization of Fenton processes through neural network and genetic algorithm

Hüseyin Cüce\*, Fulya Aydın Temel\*\*†, and Ozge Cagcag Yolcu\*\*\*

\*Department of Geomatic Engineering, Faculty of Engineering, Giresun University, Giresun, Turkey

\*\*Department of Environmental Engineering, Faculty of Engineering, Giresun University, Giresun, 28200, Turkey

\*\*\*Department of Statistics, Faculty of Sciences and Arts, Marmara University, İstanbul, 34722, Turkey

(Received 17 April 2021 • Revised 8 June 2021 • Accepted 9 June 2021)

**Abstract**—Response surface methodology (RSM), multi-layer perceptron trained by Levenberg-Marquardt (MLP-LM); multi-layer perceptron and Sigma-Pi neural networks trained by particle swarm optimization (PSO) were used to effectively and reliably predict the performance of Classical-Fenton and Photo-Fenton processes.  $H_2O_2$  doses, Fe(II) doses, and  $H_2O_2$ /Fe(II) rates were determined as independent variables in batch reactors. The performance of models was compared by using RMSE and MAE error criteria. The performance of models was also evaluated in terms of some properties of regression analysis and scatter that showed high linear relationship between the predictions of SP-PSO and the actual removal values. As a distinctive aspect of this study, SPNN trained by PSO was used for the first time in the literature in this area and the best predictive results for almost all cases were generated. Moreover, the genetic algorithm (GA) was applied for SP-PSO model results to determine the optimum values of the study. According to the results of GA, under the optimum conditions Photo-Fenton processes had higher performance in each experiment. Thereby, SP-PSO produced satisfactory prediction results without the need for any additional experiments in the case that experimental designs are difficult or costly for wastewater treatment.

Keywords: Fenton, Multilayer Perceptron, Sigma Pi Neural Network, Particle Swarm Optimization, Genetic Algorithm, Response Surface Methodology

### INTRODUCTION

The lack of water and the decreasing quality of existing water resources are concerning for today and the future [1]. It is necessary to take some measures to manage water resources effectively, to determine the usage purposes for today and the future, and to protect. As a concept of sustainable water management, recycling and reuse of wastewater applied in many countries has attracted attention recently [2,3]. Greywater, which has the potential for recycle and reuse, constitutes the majority of domestic wastewater. Wastewaters from the kitchen, bath, and laundry are named greywater. Reuse of the wastewater will support the decreasing of pollution load in the receiving environments and consequently protect water resources [4]. Laundry wastewaters in the gray water group contain surfactants, buffers, soap powders, special chemicals, bleach, heavy metals, mineral oils, paint, and other suspended solids [5-7]. Laundry wastewater generates a threat to the ecosystem and all creatures and prevents the self-cleaning process of the receiving aquatic environment [4]. To avoid these threats, it is a considerable importance for the common future to reuse wastewater, especially from commercial laundries by treating them with special treatment processes.

In the literature, the performance of some treatment methods alone or in combination has been evaluated for the treatment of

laundry wastewater, such as expanded granular sludge bed reactor-anaerobic treatment [8]; electrocoagulation/electroflotation [9,10]; microfiltration [11]; coagulation-flocculation-sedimentation-adsorption-microfiltration [12]; ultrafiltration-adsorption/nano-filtration/electro-oxidation [5]; chemical coagulation-flocculation-ultraviolet photolysis [4]; polyethersulfone/polyvinylpyrrolidone ultrafiltration membranes [13]; and electro-oxidation/electro-peroxone/ozonation [14].

Apart from all these methods, there are hardly any studies examining the treatment of laundry wastewater by Fenton-based processes. Fenton-based processes are a group of advanced oxidation processes that have been used to treat the different kinds of wastewater due to their simple operation, easy system, relevant cost, and applicability in different temperatures. The most important disadvantage of these processes is that the pollutant removal performance has decreased depending on the suspended solids content of wastewater [15,16]. Fenton reaction is a catalytic reaction between  $H_2O_2$  and Fe(II) ions in acidic pH values [17]. At the end of the Fenton reaction, nearly all organic materials in wastewater can rapidly convert under favor of the activity of  $OH^*$  radical to  $CO_2$ ,  $H_2O$ , and by-products [15,18]. Researchers have made some modifications (UV, sonic, electric current addition) to the process to minimize the negatives such as chemical cost, sludge management, and time cost encountered in the classical-Fenton process and have investigated the removal performance. In this way, Fenton and its modifications are named as photo-Fenton, electro-Fenton, sono-Fenton, photo-electro-Fenton, photo-sono-Fenton, sono-electro-Fenton, photo-Fenton/ $TiO_2$  [19-21].

†To whom correspondence should be addressed.

E-mail: fulya.temel@giresun.edu.tr

Copyright by The Korean Institute of Chemical Engineers.

Lately, some approaches have been put forward to model Fenton processes and to predict the performance of these processes that were operated under specific conditions. Most of these approaches have been statistical-based experimental models such as RSM, while ANNs that are machine learning-based models have started to be implemented lately. Although ANNs have been the focus of many studies in predicting changes as a function of time [22-24], they have taken part in a limited number of studies that modeled Fenton-based processes used in wastewater treatment such as the color removal by BBD, RSM, and ANN-GA [25], COD removal by three-layer backpropagation [26], phenol degradation by three layers ANN [27], COD removal by RSM and ANN [28], the degradation of antibiotic by ANN-GA [29], methylene blue removal by RSM and feed-forward backpropagation [30], Phenazopyridine degradation by ANN [31], As (III) and As (V) removal by ANNs [32].

In the present study, the laundry wastewater treatment was performed by Classical-Fenton and Photo-Fenton processes, the main factors affecting the COD removal performance of both Fenton processes were evaluated by using different models. RSM, which is a statistically designed experiment method, and two different MLP models, which use additional aggregation function, were utilized with different learning algorithms such as Levenberg-Marquardt and particle swarm optimization. Besides them, the point that differentiates this study from the current studies, PSO-trained Sigma-Pi NN was applied for the first time in the literature. MLP and SP trained by PSO models presented in this study that have superior features of both RSM and NNs are the first models in the literature to apply RSM and NNs together. Moreover, the application of MLP-PSO and SP-PSO prediction models for COD removal will be a new advance to decrease the number of experiments, to determine the optimum operating conditions, to evaluate and to compare the removal performance of Fenton processes.

The scope of the study includes evaluating the model prediction performance by the root mean square error (RMSE) and mean absolute error (MAE) error criteria; detecting the performance of the best model by regression analysis, determining the behavior of the dependent variable more effectively and reliably, emphasizing the generalized ability of models via training, validation, and test, to find optimal independent values by genetic algorithm to do a comparison of model results.

## MATERIALS AND METHODS

### 1. Wastewater

The wastewater used in this study was obtained from a company that washes clothes in Nevşehir/Turkey. The laundry wastewater samples were collected as a two hour composite and accumulated in 5 L PE bottles. The collected samples were transferred with a storage box to the laboratory. The main properties of wastewater were determined according to Standard Methods [33], and they are given in Table 1. The samples were stored in the refrigerator at 4 °C.

### 2. The Experimental Procedures of Classical and Photo-Fenton Processes

The experiments of the Classical-Fenton process were performed

**Table 1. The main properties of laundry wastewater samples**

Parameters	Values
pH	8
Temperature (°C)	21
Conductivity (µs/cm)	3,400
Dissolved oxygen (mg/L)	6.21
Color (436 nm)	1,303
Color (525 nm)	1,080
Color (620 nm)	911
COD (mg/L)	1,077
Sulfate (mg/L)	1,674.8
Ortho-phosphate (mg/L)	0.59
Anionic surfactant (mg/L)	1.59



**Fig. 1. A schematic representation of Photo-Fenton process.**

in 500 mL of the reactors by using a Jar Test Flocculator (Velp JLT6). The experiments of the Photo-Fenton process were conducted in a light-proof wooden cabin that was 50 cm×50 cm×42 cm (L×W×H). The cabin included UV-C radiation lamps of 8 watts that were located parallelly, 500 mL of the reactors, and two magnetic stirrers (Mtops MS200). A schematic representation is given in Fig. 1. The experiments were carried in a batch system at room temperature by using 200 mL of laundry wastewater for both processes. Fenton reagents were prepared by using  $\text{FeSO}_4 \cdot 7\text{H}_2\text{O}$  and  $\text{H}_2\text{O}_2$  (30%, w/w). NaOH or  $\text{H}_2\text{SO}_4$  solutions were used to adjust the pH value of wastewater. Sampling and experimental materials were cleaned by using distilled water and 5% of  $\text{HNO}_3$  solution. All chemicals used in the present study were analytical grade. COD removal efficiencies were determined as functions of Fe(II) dose,  $\text{H}_2\text{O}_2$  dose, and  $\text{H}_2\text{O}_2/\text{Fe(II)}$  rates in both Fenton processes. The mixing of wastewater and reagents in both systems was operated in first fast mixing of 300 rpm and then a slow mixing of 90 rpm. The fast mixing was only two minutes for both of them, but the slow mixing occupied 45 minutes and 20 minutes for Classical-Fenton and Photo-Fenton experiments, respectively.

After precipitation, the mixture was filtered by using 0.45 µm of membrane filters. COD concentration in the supernatants was done by closed reflux method by using a thermoreactor (Hach LT200)

and a spectrophotometer (Hach DR3900) according to the standard method [33]. pH and electrical conductivity were determined by using a multi-meter during experiments (Hach HQ40d). COD removal efficiency (RE, %) was found by Eq. (1) obtained from inlet COD concentration ( $C_i$ , mg/L) and final COD concentration ( $C_f$ , mg/L).

$$RE(\%) = \frac{C_i - C_f}{C_i} \times 100 \quad (1)$$

### 3. The Multilayer Perceptron Neural Networks (MLP)

Artificial neural network (ANN), shown to be effective alternatives to traditional statistical techniques, is an interconnected group of neurons using mathematical transactions to process information. Multilayer perceptron neural networks are one of the most popular self-adaptive architectures which can change their structure based on inputs and outputs information. The first study of MLP was introduced by Werbos [34]. Just like the other ANN models which mimic the human brain working principle, MLP's learning ability depends on learning algorithms. Basically, MLP has three layers as input, hidden and output layers with several neurons. All the neurons in the sequential layers are connected with each other with the intention of solving nonlinear problems by taking advantage of its data-driven feature. The aggregation function used in the neurons and the selected learning algorithm has a significant effect on the performance of the MLP. It has a huge usage area thanks to its structural flexibility and well-representational capabilities features. In this study, MLP which is widely used in many fields due to its learning and generalization capabilities, was used with training by the Levenberg-Marquardt training algorithm (MLP-LM). If the network structure of MLP-LM is not carefully selected, the MLP-LM algorithm can get stuck in a local minimum or it might lead to slow convergence or even network failure. Different kinds of artificial intelligence optimization techniques have been utilized to overcome these problems. In the present study, the particle swarm optimization (PSO) algorithm, a population-based algorithm that can provide the best possible solutions to different math problems using nature-inspired techniques, was preferred for the training of ANN. And MLP was used with training by PSO as second.

### 4. Sigma-Pi Neural Network (SPNN)

The Sigma-Pi neural network has the ability of fast learning, which reduces the network complexity by using efficient polynomials for many input layer variables. It has been introduced by Shin and Gosh [35]. The number of linear combinations obtained from the sum of the units found in the hidden layer represents the degree of SPNN. The features of having both additive and multiplicative aggregation functions make SPNN more flexible. In the structure of it, the input layer connects with the hidden layer and the hidden layer outputs are fed to the output layer. SPNN contains weights fixed to unity lying between the hidden layer and output layer, which reduces also the training time. Especially, it is quite easier to determine nonlinear relations between the inputs and the outputs. When compared to multilayer perceptron, an important advantage of the Sigma-Pi neural network is that it requires fewer weights and neurons and has a lower number of computations. So, it can be clearly emphasized that it is superior to MLP models

in terms of these features. The output of the SPNN is calculated by using the following formulas:

$$h_j = f_1 \left( \sum_{i=1}^N w_{ij} X_i + b_j \right) \quad (2)$$

$$\hat{y} = f_2 \left( \prod_{j=1}^K h_j \right) \quad (3)$$

Here  $w_{ij}$  ( $i: 1, 2, \dots, N, j: 1, 2, \dots, K$ ) represents the weights and  $b_j$  represents the biases. While  $h_j$  shows the output of the  $j^{\text{th}}$  hidden layer neuron,  $f_1$  and  $f_2$  depict the linear and logistic activation functions, respectively.

### 5. Particle Swarm Optimization (PSO)

PSO is a population-based heuristic algorithm that replicates the behavior of natural flocks such as shoals and flocks of birds. And it was first proposed by Kennedy and Eberhart [36]. The distinguishing feature of this heuristic algorithm can be summarized as the ability to obtain a global optimum solution by simultaneously examining different points in different regions of the solution space. So, having this feature gives the opportunity for PSO algorithm to reach a global optimum by escaping the local optimum. The main parameters of this method are the inertia and acceleration of a particle that is iteratively adapted during the exploration process. In this study, the modified particle swarm optimization (MPSO) method was utilized to get the optimal parameters for the SPNN from the training process.

### 6. Genetic Algorithm (GA)

A genetic algorithm is a search algorithm that is inspired by Darwin's theory of natural evolution. The difference between traditional algorithms and GA is that GA is not static but dynamic as it can evolve over time. While GA was first introduced by Holland [37], Goldberg [38] improved it to get better search results. GA mimics the natural evolution process by modifying a population of individual solutions to find beneficial solutions to complicated problems. GA consists of basic processes such as natural selection, mutation, and crossover. The search process begins by creating random solutions (individuals) that are each containing several features (chromosomes). Individuals are evaluated in terms of fitness function values. Then, cross-over and mutation transactions are performed by taking into consideration the laws of genetics. Thus, new generations are created subsequently until obtaining satisfactory search results.

## RESULTS AND DISCUSSION

In the present study, different ANN models were analyzed to be able to predict the main factors affecting the removal performance of both Fenton processes for the treatment of laundry wastewater. For this purpose, first the effect of the MLP-LM model was investigated. And based on the idea of the effect of the training algorithm on the system, PSO-trained MLP results, which are not derivative-based and have a more flexible structure, were evaluated. In addition, getting the results from SPNN gave the opportunity to enhance prediction performance by taking advantage of the features of SPNN for the first time in this field. Owing to the ability to combine both additive and multiplicative aggregation func-

**Table 2. The experimental conditions and architectures of neural networks**

Exp. No	Fenton process	Independent variables	Fixed variables	NNs architecture
1	Classic	A. Fe(II) dose (50-400 mg/L) B. H <sub>2</sub> O <sub>2</sub> dose (300 mg/L, 900 mg/L)	1. pH/3 2. Temperature/23±2 °C 3. Fast mixing speed/300 rpm 4. Slow mixing speed/90 rpm	from 2-1-1 to 2-4-1
2	Photo	A. Fe(II) dose (50-400 mg/L) B. H <sub>2</sub> O <sub>2</sub> dose (600 mg/L, 900 mg/L)	1. pH/3 2. Temperature/23±2 °C 3. Fast mixing speed/300 rpm 4. Slow mixing speed/90 rpm	from 2-1-1 to 2-4-1
3	Classic	A. H <sub>2</sub> O <sub>2</sub> dose (150-1,080 mg/L) B. Fe(II) dose (150 mg/L, 300 mg/L, 400 mg/L)	1. pH/3 2. Temperature/23±2 °C 3. Fast mixing speed/300 rpm 4. Slow mixing speed/90 rpm	from 2-1-1 to 2-4-1
4	Photo	A. H <sub>2</sub> O <sub>2</sub> dose (300-900 mg/L) B. Fe(II) dose (150 mg/L, 200 mg/L, 400 mg/L)	1. pH/3 2. Temperature/23±2 °C 3. Fast mixing speed/300 rpm 4. Slow mixing speed/90 rpm	from 2-1-1 to 2-4-1
5	Classic	A. H <sub>2</sub> O <sub>2</sub> dose (150-1,080 mg/L) B. Fe(II) dose (50-400 mg/L)	1. pH/3 2. Temperature/23±2 °C 3. Fast mixing speed/300 rpm 4. Slow mixing speed/90 rpm	from 2-1-1 to 2-4-1
6	Photo	A. H <sub>2</sub> O <sub>2</sub> dose (300-900 mg/L) B. Fe(II) dose (50-400 mg/L)	1. pH/3 2. Temperature/23±2 °C 3. Fast mixing speed/300 rpm 4. Slow mixing speed/90 rpm	from 2-1-1 to 2-4-1
7	Classic	A. Contact time (0-60 min) B. H <sub>2</sub> O <sub>2</sub> dose (600 mg/L, 900 mg/L)	1. pH/3 2. Temperature/23±2 °C 3. Fast mixing speed/300 rpm 4. Slow mixing speed/90 rpm 5. Fe(II) dose/400 mg/L	from 2-1-1 to 2-4-1
8	Photo	A. Contact time (0-60 min) B. H <sub>2</sub> O <sub>2</sub> dose (600 mg/L)	1. pH/3 2. Temperature/23±2 °C 3. Fast mixing speed/300 rpm 4. Slow mixing speed/90 rpm 5. Fe(II) dose/400 mg/L	from 2-1-1 to 2-4-1

tions, SPNN performed quite better for determining nonlinear relations between the inputs and the outputs. The datasets were divided into three subsets as training, validation, and testing. From this point, H<sub>2</sub>O<sub>2</sub> doses, Fe(II) doses, and H<sub>2</sub>O<sub>2</sub>/Fe(II) rates were determined as independent variables/inputs of the prediction models for each experiment. Moreover, the RSM method was also applied to evaluate the experiments from a statistical perspective for each of the experiments. Through a genetic algorithm, optimal values belonging to independent variables were also obtained by using the prediction results put forward by the SPNN model which depicts the best prediction performance. And a comprehensive comparison was made to be able to discuss all the obtained results with different perspectives. Analysis and modelling using all ANNs were performed with the MATLAB R2018b program codes created by

researchers. The experimental properties of Classical-Fenton and Photo-Fenton Processes are listed in Table 2. A scheme of the combination of ANNs and genetic algorithms is given in Fig. 2.

### 1. Evaluation Criteria

In this study, the obtained prediction results through four models were evaluated from different perspectives. First, the most widely used RMSE and MAE criteria were discussed. Here, the MAE criterion was preferred in addition to RMSE since this criterion is quite useful for revealing the prediction performance of models as it gives a measure of the percentage of error. The formulas of two measures can be given with Eqs. (4) and (5).

$$RMSE = \sqrt{\frac{1}{n} \sum_{p=1}^n (\text{Target}_p - \text{Output}_p)^2} \quad (4)$$

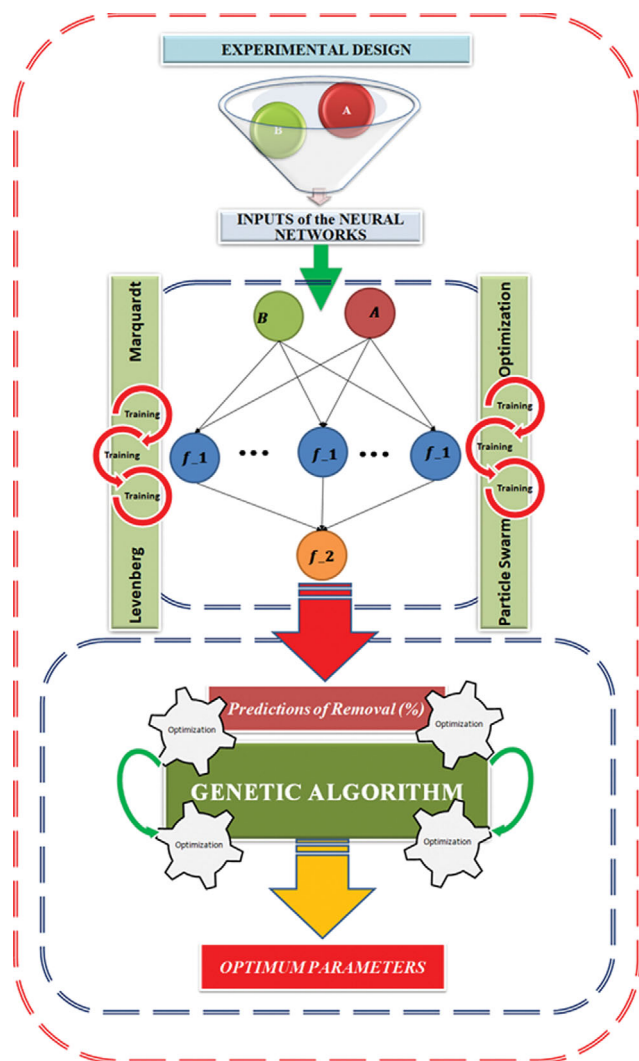


Fig. 2. A scheme of the combination of ANNs and genetic algorithms.

$$\text{MAE} = \text{mean}(|\text{Target}_p - \text{Output}_p|), p=1, 2, \dots, n \quad (5)$$

In a second way, regression models were obtained for the predictions and target values. The regression model is given by Eq. (6). To be able to talk about a successful prediction tool, the regression and determination coefficients of the model are expected to be equal to 1 or quite close to 1.

$$Y_i = \beta \hat{Y}_i + \varepsilon_i \quad (6)$$

And finally, a scatter diagram that shows the degree of harmony of the obtained predictions with the removal efficiency was presented as another performance evaluation indicator.

## 2. Modelling

### 2-1. RSM Modelling

As a traditional statistical model, RSM was performed to model COD removal performance of Classical and Photo-Fenton Processes for laundry wastewater treatment. Since RSM has been the most widely used statistical method in this field, basic information about it was given in this study. The structure of the second-order polynomial model for the case where there are  $k$  independent variables is represented by Eq. (7).

$$\text{RE}(\%) = \beta_0 + \sum_{i=1}^k \beta_i X_i + \sum_{i=1}^k \beta_{ii} X_i^2 + \sum_{i=1}^k \sum_{j=1, j \neq i}^k \beta_{ij} X_i X_j + \varepsilon \quad (7)$$

For all experiment designs including Classical-Fenton and Photo-Fenton Processes, the results of the observed data in terms of un-coded factors employing RSM are given in Table 3. When RSM results given in Table 3 are considered, in terms of MAE, it was observed that RSM produced predictions with error higher than 2% except experiments 7 and 8. While MAE values were around 3% in Experiments 1 and 5 (Classical-Fenton process), these values were obtained by nearly 5% in Experiments 2 and 6 (Photo-Fenton process). As for RMSE, RSM produced results with error nearly 3% and higher than 3% except Experiments 7 and 8. Experiments 2 and 6 (Photo-Fenton process), in particular, were the ones in which RSM performed the worst with approximately 6% error. Moreover, as another measure of the success of the method,  $R^2$  values were produced as relatively high values (higher than 90%) for all experiments.

### 2-2. ANN Modelling

Neural networks (NNs) play an important role in many areas, bringing us to the next level in artificial intelligence thanks to their interdisciplinary approach. In this study, the basic aim is to predict the laundry wastewater treatment performed by Classical-Fenton and Photo-Fenton processes through different ANN models. The utilized first model is MLP trained with Levenberg-Marquardt learning algorithm. Secondly, MLP trained by PSO was used to be able to consider the learning algorithms' effect on the performance of the system. Moreover, SPNN model was implemented for eight different data sets, taking advantage of having both additive and

Table 3. The results of RSM for experiments

Exp. No	Fenton	Obtained model (by omitting insignificant terms)	$R^2$ (%)	RMSE	MAE (%)
1	Classic	$\widehat{\text{RE}} = 11.61 + 0.2032A - 0.00594B + 0.000322A^2 + 0.000112AB$	95.16	3.8216	3.0863
2	Photo	$\widehat{\text{RE}} = -3.8 + 0.533A - 0.000686A^2$	93.93	5.9167	4.7506
3	Classic	$\widehat{\text{RE}} = 11.2 + 0.0637A + 0.1064B - 0.000068A^2 + 0.000171AB$	94.80	3.5694	2.9654
4	Photo	$\widehat{\text{RE}} = -163.9 + 0.2061A + 1.3251B - 0.000152A^2 - 0.002064B^2$	97.70	2.8686	2.2445
5	Classic	$\widehat{\text{RE}} = -0.77 + 0.0790A + 0.1663B - 0.000065A^2 - 0.000254B^2 + 0.000108AB$	93.68	4.2914	3.5048
6	Photo	$\widehat{\text{RE}} = -71.7 + 0.1769A + 0.6100B - 0.000105A^2 - 0.000766B^2$	93.03	5.8615	4.7700
7	Classic	$\widehat{\text{RE}} = 6.72 + 1.265A + 0.0067B - 0.01333A^2 + 0.000726AB$	98.91	1.9269	1.5278
8	Photo	$\widehat{\text{RE}} = -27.45 + 2.062A + 0.1166B - 0.01229A^2 - 0.000077B^2$	99.84	0.9953	0.6763

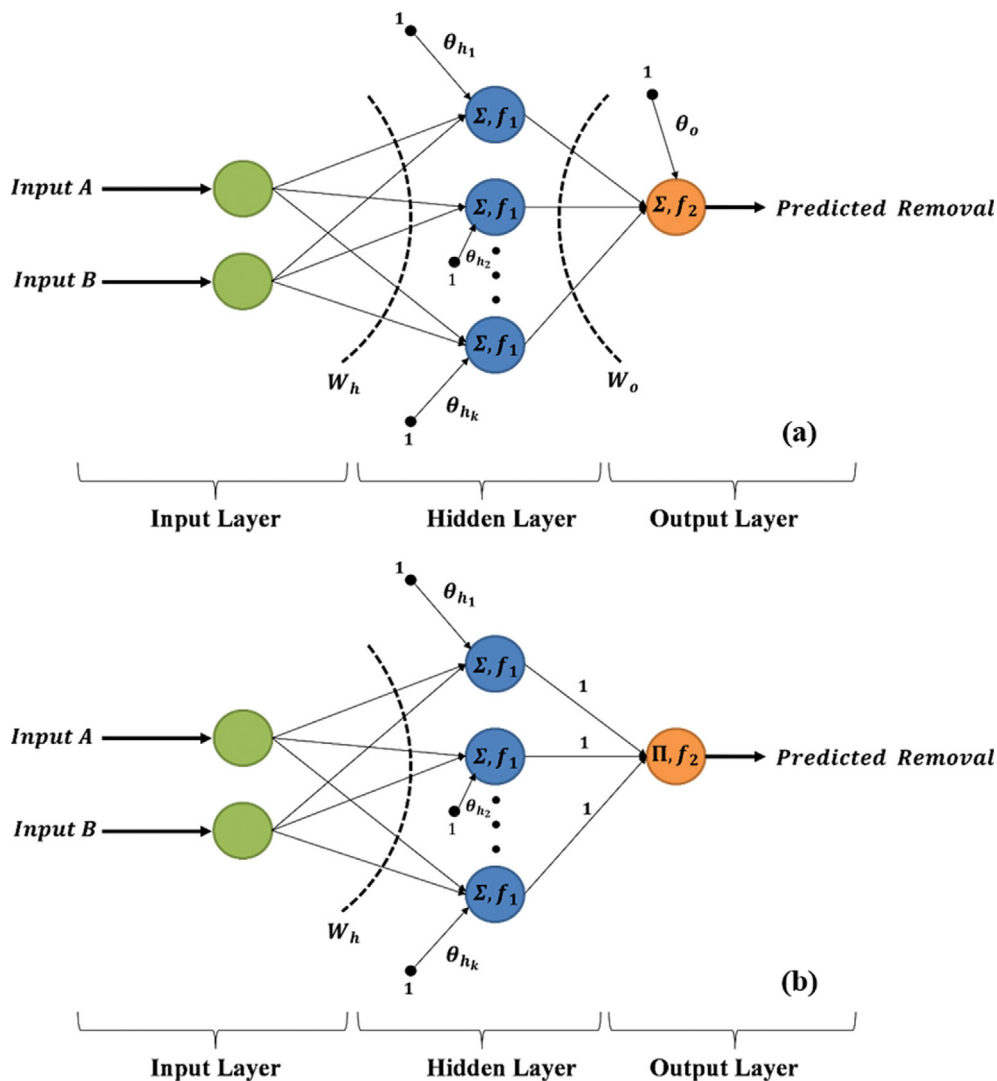


Fig. 3. Illustrations of MLP structure (a) and SPNN structure (b)/2-k-1 Architecture.

multiplicative aggregation functions. Compared to MLP models, SPNN model used requires fewer weights and neurons with fewer computations. And the structure of SPNN gives the opportunity to get better predictive results for nonlinear relationships as well as linear relationships. Also in this study, SPNN was trained by PSO in order to benefit from this heuristic algorithm. So abovementioned second (MLP-PSO) and third model (SP-PSO) had the priority and distinguishing features of being the first performed prediction model in this area. MLP and SPNN structures are presented with Fig. 3(a) and 3(b), respectively.

Table 4 and Table 5 represent the obtained prediction results belonging to these three alternative ANN models (MLP-LM, MLP-PSO, and SP-PSO) for laundry wastewater treatment performed by Classical-Fenton and Photo-Fenton processes. And results are given in terms of RMSE and MAE criteria for all experiment designs.

When Tables 4 and Table 5 are examined in detail, it is obvious that the prediction performance of ANN-based models is better than RSM in terms of both criteria for all cases. Comparing three ANN-based models, SP-PSO produced the best prediction results,

as expected, according to the average success rankings created for both criteria. The reason behind this situation is mainly due to SPNN's ability to use both additive and multiplicative addition functions in the analysis process. Thanks to this feature, SPNN model is more proper for the types of problems with non-linearity dominance. Moreover, PSO learning algorithm has a positive effect on the SPNN's performance as there is no problem of being stuck in the local optimum. It was clear that, in this study for all experiments, SP-PSO produced predictive results with around 1% error and in many cases lower than this rate in terms of both evaluation criteria. Along with all these features, the obtained prediction results also emphasize the superiority of SP-PSO. From a different perspective, unlike RSM, ANN-based prediction tools managed to produce stronger results in terms of reliability and consistency by analyzing the data in different parts such as training, validation, and test sets. Obtaining 1% or fewer MAE values can be seen as concrete proof of this.

In the light of all these results, it can be emphasized as a general conclusion that while ANN-based methods yielded better results

**Table 4. The prediction results in terms of RMSE**

Case	Processes	# Samples	RSM		SP-PSO		MLP-PSO		MLP-LM		
			RMSE	Rank	RMSE	Rank	RMSE	Rank	RMSE	Rank	
Effect of Fe (II) doses	Classical-Fenton	10	Training	----	----	0.5609	1	1.0304	2	1.1121	3
		3	Validation	----	----	0.9487	1	1.0211	2	1.1053	3
		3	Test	----	----	0.6134	1	1.4239	2	1.8213	3
		16	ALL	3.8216	4	0.6603	1	1.1132	2	1.2744	3
	Photo-Fenton	10	Training	----	----	0.6048	1	1.9812	2	2.6711	3
		3	Validation	----	----	0.8568	1	3.0619	2	3.2987	3
		3	Test	----	----	0.6055	1	0.7951	2	0.8792	3
		16	ALL	5.9167	4	0.6596	1	2.0808	2	2.5777	3
Effect of H <sub>2</sub> O <sub>2</sub> doses	Classical-Fenton	11	Training	----	----	1.4220	1	1.8162	2	1.9560	3
		4	Validation	----	----	1.5408	1	2.0940	2	2.3768	3
		4	Test	----	----	1.6857	2	1.5728	1	1.7467	3
		19	ALL	3.5694	4	1.5062	1	1.8313	2	2.0116	3
	Photo-Fenton	11	Training	----	----	1.0259	1	3.2656	2	3.8111	3
		4	Validation	----	----	0.7960	1	3.1481	2	4.1365	3
		4	Test	----	----	0.7034	1	1.3853	3	1.2619	2
		21	ALL	2.8686	2	0.9308	1	2.9757	3	3.5431	4
Effect of H <sub>2</sub> O <sub>2</sub> /Fe(II)	Classical-Fenton	20	Training	----	----	1.0825	1	2.9775	3	2.7421	2
		5	Validation	----	----	0.9007	1	2.7463	2	3.0036	3
		5	Test	----	----	1.2094	1	1.6666	2	1.7252	3
		30	ALL	4.2914	4	1.0771	1	2.7623	3	2.6481	2
	Photo-Fenton	21	Training	----	----	1.2036	1	2.8765	2	3.3182	3
		5	Validation	----	----	1.1194	1	3.2038	3	2.0870	2
		5	Test	----	----	1.3011	1	1.5805	2	1.6065	3
		31	ALL	5.8615	4	1.2069	1	2.7683	2	2.9287	3
Effect of contact time	Classical-Fenton	10	Training	----	----	1.2148	1	1.6957	3	1.6848	2
		2	Validation	----	----	1.7752	2	1.8478	3	1.7479	1
		2	Test	----	----	0.2228	1	0.3167	2	0.3897	3
		14	ALL	1.9269	4	1.2294	1	1.5987	3	1.5766	2
	Photo-Fenton	5	Training	----	----	1.0261	1	2.7793	3	1.9898	2
		2	Validation	----	----	0.6110	1	3.4225	3	1.4124	2
		2	Test	----	----	0.1310	1	0.6499	3	0.4291	2
		9	ALL	0.9953	2	0.8196	1	2.6435	4	1.6383	3
Average			Training	----		1.0000		2.3750		2.6250	
			Validation	----		1.1250		2.3750		2.5000	
			Test	----		1.1250		2.1250		2.7500	
			ALL	3.5000		1.0000		2.6250		2.8750	

than RSM, which is a classical method, ANN models which used PSO algorithm in the training process had a more effective performance. Furthermore, it is observed that the SP-PSO model has much better prediction results, comparing PSO-based MLP, in terms of both criteria. So, these results indicate that SP-PSO can produce satisfactory prediction results without the need for any additional experiments even in the case that experimental designs are difficult or costly.

The other aspect to examine the superior prediction ability of any tool is to set up a simple linear regression model which is constituted between predictions and target values. From this point of

view, it was evaluated SMN-PSO which showed outstanding performance among the other models. To be able to talk about a satisfactory and applicable prediction tool, the estimate of the regression coefficient ( $\beta$ ) and also the determination coefficient ( $R^2$ ) of the model  $Y_i = \beta \hat{Y}_i + \varepsilon_i$  are desired to be 1 or quite close to 1. The obtained results from the regression analyses are presented in Table 6.

The results obtained from the regression analysis were evaluated separately in accordance with three evaluation criteria. For all data sets, the findings given in Table 6 represented that both  $\beta$  and  $R^2$  values were fairly close to 1 just as expected. It was proof that SP-PSO's prediction results were quite close to actual values. Get-

**Table 5. The prediction results in terms of MAE**

Case	Processes	# Samples	RSM		SP-PSO		MLP-PSO		MLP-LM		
			MAE	Rank	MAE	Rank	MAE	Rank	MAE	Rank	
Effect of Fe (II) doses	Classical-Fenton	10	Training	----	----	0.4540%	1	0.9075%	3	0.6886%	2
		3	Validation	----	----	0.8281%	2	0.8547%	3	0.6540%	1
		3	Test	----	----	0.5830%	1	1.4013%	3	1.1851%	2
		16	ALL	3.0863%	4	0.5484%	1	0.9902%	3	0.7752%	2
	Photo-Fenton	10	Training	----	----	0.5271%	1	1.6070%	2	1.9073%	3
		3	Validation	----	----	0.8321%	1	2.3520%	2	3.0609%	3
		3	Test	----	----	0.4945%	1	0.6240%	2	0.6928%	3
		16	ALL	4.7506%	4	0.5782%	1	1.5624%	2	1.8959%	3
Effect of H <sub>2</sub> O <sub>2</sub> doses	Classical-Fenton	11	Training	----	----	1.1791%	1	1.3272%	2	1.3841%	3
		4	Validation	----	----	1.1887%	1	1.7239%	2	2.1232%	3
		4	Test	----	----	1.2882%	2	1.1941%	1	1.5378%	3
		19	ALL	2.9654%	4	1.2041%	1	1.3827%	2	1.5721%	3
	Photo-Fenton	11	Training	----	----	0.7411%	1	2.7251%	3	2.6410%	2
		4	Validation	----	----	0.6595%	1	2.3576%	2	3.1227%	3
		4	Test	----	----	0.5871%	1	1.3154%	3	1.0778%	2
		21	ALL	2.2445%	2	0.6963%	1	2.3866%	3	2.4350%	4
Effect of H <sub>2</sub> O <sub>2</sub> /Fe(II)	Classical-Fenton	20	Training	----	----	0.9398%	1	2.2443%	3	2.1655%	2
		5	Validation	----	----	0.7888%	1	2.5383%	3	2.3164%	2
		5	Test	----	----	1.0930%	1	1.1906%	2	1.4780%	3
		30	ALL	3.5048%	4	0.9401%	1	2.1177%	3	2.0761%	2
	Photo-Fenton	21	Training	----	----	1.0478%	1	2.4705%	3	2.3483%	2
		5	Validation	----	----	0.9782%	1	2.9999%	3	1.6101%	2
		5	Test	----	----	0.9490%	1	1.2478%	2	1.3030%	3
		31	ALL	4.7707%	4	1.0206%	1	2.3587%	3	2.0607%	2
Effect of contact time	Classical-Fenton	10	Training	----	----	0.8531%	1	1.4434%	3	1.3003%	2
		2	Validation	----	----	1.7457%	3	1.6490%	2	1.4249%	1
		2	Test	----	----	0.2143%	1	0.2262%	2	0.3650%	3
		14	ALL	1.5278%	4	0.8893%	1	1.2989%	3	1.1845%	2
	Photo-Fenton	5	Training	----	----	0.9463%	1	2.4083%	3	1.6205%	2
		2	Validation	----	----	0.6009%	1	2.9851%	3	1.2806%	2
		2	Test	----	----	0.0969%	1	0.5705%	3	0.3257%	2
		9	ALL	0.6763%	1	0.6808%	2	2.1281%	3	1.2573%	2
Average			Training	----		1.0000		2.7500		2.2500	
			Validation	----		1.3750		2.5000		2.1250	
			Test	----		1.1250		2.2500		2.6250	
			ALL	3.3750		1.1250		2.7500		2.5000	

**Table 6. The results of the regression analysis for SP-PSO predictions**

Exp. No	Process	# Samples	$Y = \hat{\beta} Y_{pre}$	95% Confidence interval of $\beta$		R <sup>2</sup> %
				Lower bound	Upper bound	
1	Classical-Fenton	16	$Y = 1.003834 Y_{pre}$	0.997080	1.010588	99.9851
2	Photo-Fenton	16	$Y = 0.999695 Y_{pre}$	0.994247	1.005143	99.9902
3	Classical-Fenton	19	$Y = 0.999051 Y_{pre}$	0.987377	1.010725	99.9443
4	Photo-Fenton	21	$Y = 0.996580 Y_{pre}$	0.991005	1.002155	99.9856
5	Classical-Fenton	30	$Y = 0.998325 Y_{pre}$	0.991291	1.005360	99.9656
6	Photo-Fenton	31	$Y = 1.000197 Y_{pre}$	0.993808	1.006587	99.9707
7	Classical-Fenton	14	$Y = 1.012887 Y_{pre}$	0.999870	1.025924	99.9540
8	Photo-Fenton	9	$Y = 1.005438 Y_{pre}$	0.996606	1.014270	99.9884



ting the determination coefficient,  $R^2$ , nearly 1 for each experiment showed the high linear relationship between the predictions of SP-PSO and the actual removal values. On the other 95% confidence intervals of  $\beta$  covered 1 and also had a very narrow frame. In light of all this information, it is clear that SP-PSO can be used as an effective estimation tool.

When the results were considered from a different perspective, in addition to statistical evaluations, to show visual demonstration for the superior performance of SP-PSO, scatter diagrams were presented. In a scatter plot which is the mathematical diagram using Cartesian coordinates displaying the observed and predicted removal efficiency values, most of the points need to be close to

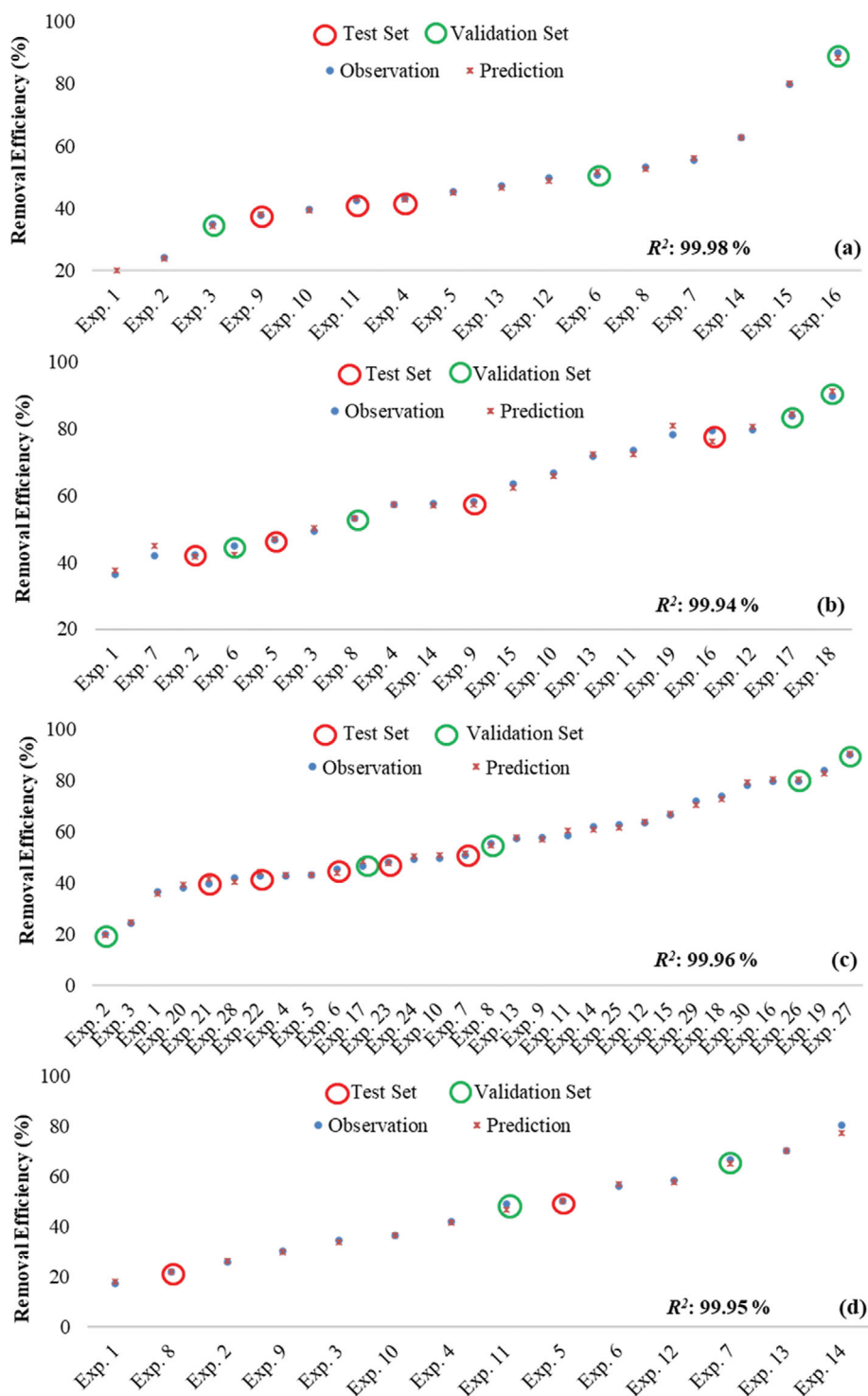


Fig. 4. The visual evaluation of observations and predictions for the entire data from Classical-Fenton experiments ((a) Exp. 1; (b) Exp. 3; (c) Exp. 5; (d) Exp. 7).

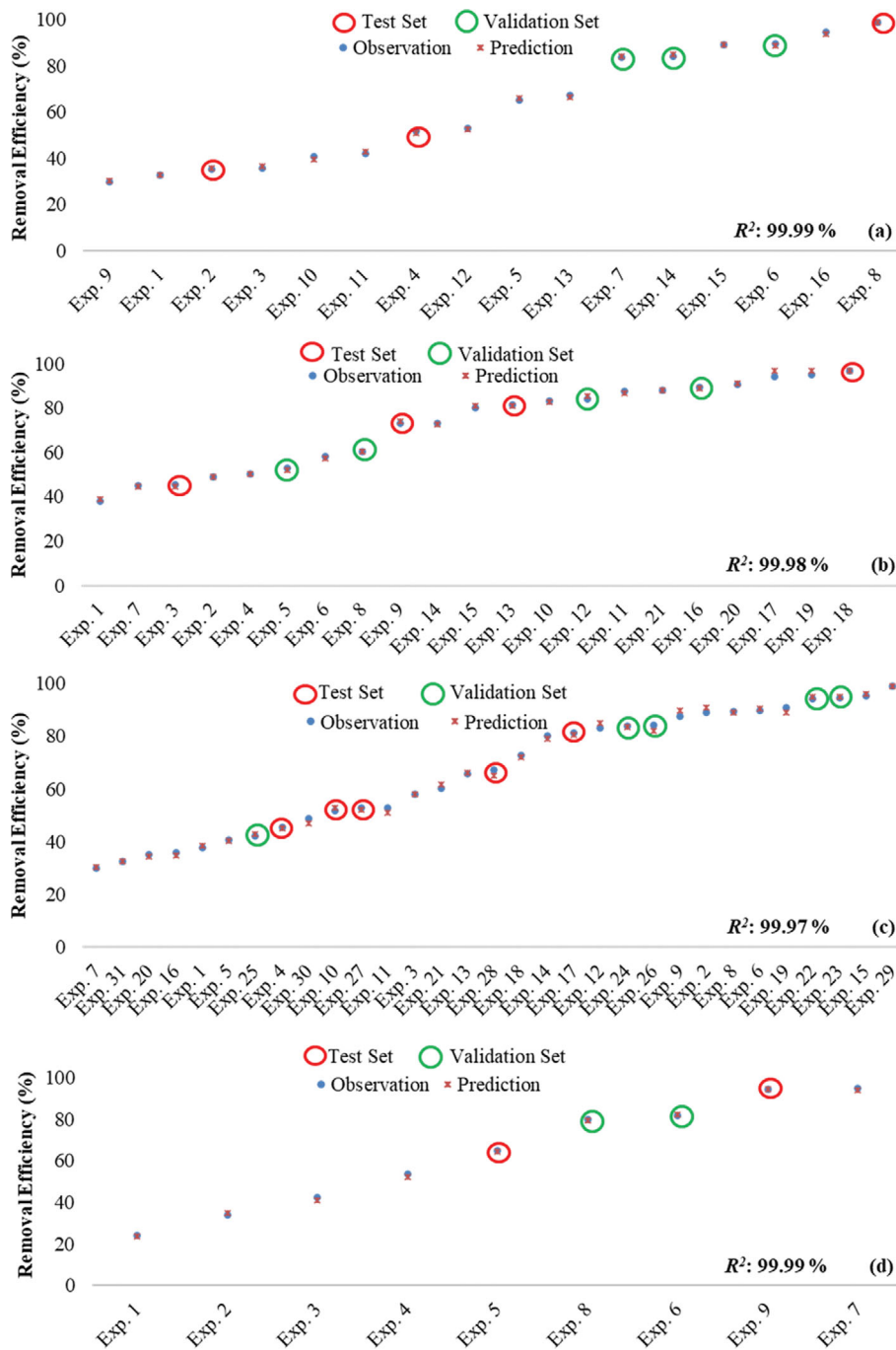


Fig. 5. The visual evaluation of observations and predictions for the entire data from Photo-Fenton experiments ((a) Exp. 2; (b) Exp. 4; (c) Exp. 6; (d) Exp. 8).

the line segment. The obtained scatter graphs are depicted in Fig. 4 and 5. And it demonstrated that most of the points on the scatter plots were in proximity to the line segment, as expected for the best prediction tools.

Moreover, for each experiment, the high degree of harmony of the predictions produced by SP-PSO with the observed removal values is illustrated by Fig. 4 and 5. This harmony can be seen as another indicator of the excellent performance of the SP-PSO. When the figures are carefully examined, it is seen that the markers rep-

resenting the observations and predictions are placed almost on top of each other. This means that the prediction error is nominal and negligible.

### 3. Parameters Optimization via Genetic Algorithm

In this section, genetic algorithm was performed to be able to determine optimal values of each independent variable in the wastewater treatment. In addition to obtaining optimal values for each experiment, it is also possible to get an idea of the performance of Photo-Fenton processes compared to Classic-Fenton using GA.

**Table 7. The data of the optimization process**

Exp. No	Process	Constraints	Optimal values	Objective function values	Desirability (%)
1	Classical-Fenton	50≤Fe(II) mg/L≤400 300≤H <sub>2</sub> O <sub>2</sub> mg/L≤900	400 900	89.3319	99.23
2	Photo-Fenton	50≤Fe(II) mg/L≤400 600≤H <sub>2</sub> O <sub>2</sub> mg/L≤900	400 899.9692	98.9853	99.95
3	Classical-Fenton	150≤Fe(II) mg/L≤400 150≤H <sub>2</sub> O <sub>2</sub> mg/L≤1080	992.7675 396.5552	86.8856	94.43
4	Photo-Fenton	150≤Fe(II) mg/L≤400 300≤H <sub>2</sub> O <sub>2</sub> mg/L≤900	583.4585 393.7899	96.9499	100.00
5	Classical-Fenton	50≤Fe(II) mg/L≤400 150≤H <sub>2</sub> O <sub>2</sub> mg/L≤1080	965.3792 399.9997	89.7568	99.84
6	Photo-Fenton	50≤Fe(II) mg/L≤400 300≤H <sub>2</sub> O <sub>2</sub> mg/L≤900	605.7577 399.9996	99.0173	100.00
7	Classical-Fenton	5≤t (min)≤400 600≤H <sub>2</sub> O <sub>2</sub> mg/L≤900	60 900	77.2911	94.78
8	Photo-Fenton	5≤t (min)≤60 300≤H <sub>2</sub> O <sub>2</sub> mg/L≤900	60 900	94.3350	99.38

With this aim, the output produced by SPNN corresponding to the independent variable values was used as objective function values for the genetic algorithm. As a working principle of GA, it was aimed to find optimum independent variables values that maximize the removal efficiency rate. Generally, the objective function intended to be maximized is presented as in Eq. (8).

$$y = f(X_1, X_2) \quad (8)$$

Here  $X_1$  and  $X_2$  represent the independent variables like H<sub>2</sub>O<sub>2</sub> doses, Fe(II) doses, and H<sub>2</sub>O<sub>2</sub>/Fe(II) rates, and also  $y$  depicts the removal performance of Classical and Photo-Fenton Processes from laundry wastewater. In this study, the optimization process was performed for only the SP-PSO which showed the highest prediction performance among the three NN-based prediction models. Eq. (9) represents the used objective function for 2-2-1 architecture structure. The data of the optimization process for each experiment is presented in Table 7.

$$y = f\left(\frac{1}{1 + \exp(-((X_1 \times w_{11} + X_2 \times w_{21} + b_1)(X_1 \times w_{12} + X_2 \times w_{22} + b_2)))}\right) \quad (9)$$

An important advantage of the use of NN methods in modeling such data obtained from experiments is that being able to give results even for parameters that were not tested in the experiment. When the results given in Table 6 are examined in detail, for experiment 3 with 396.5552 mg/L of Fe(II) dose and 992.7675 mg/L of H<sub>2</sub>O<sub>2</sub> dose, the optimized condition leads to maximum removal performance (86.89%) with 94.43% desirability. This is also a concrete indicator of achieving high efficiency at different parameter values for untested experiments. On the other hand, for Experiment 4, the maximum desirability was obtained (100.00%) for the optimized condition with the 393.7899 mg/L of Fe(II) dose and 583.4585 mg/L of H<sub>2</sub>O<sub>2</sub> dose. Table 6 also gives the other important information relevant to the difference between Photo-Fenton and Classical-Fenton processes on removal performance. When

the obtained results of the optimization transaction were evaluated in detail it was observed that under the optimum conditions Photo-Fenton processes have higher performance for the treatment of laundry wastewater in each experiment.

#### 4. Comparison of the Results

This study presents the prediction results produced by three NN-based prediction models as well as the results obtained from RSM for the prediction of COD removal performance of Classical and Photo-Fenton Processes in the treatment of laundry wastewater. When the results of eight different experiments were considered together and in detail, it was concluded that the NN-based models have a better predictive ability than RSM. These findings can be clearly seen from the graphs given in Fig. 6, which show the prediction performance of the models in terms of RMSE and MAE criteria for all data sets. When NN-based models were evaluated, SP-PSO exhibited the highest prediction performance. Moreover, the average success rankings of the prediction models in each experiment were considered and the findings are visualized in Fig. 7. According to these findings, SP-PSO offered the highest prediction performance for training, test, and validation data sets as well as all of the data.

## CONCLUSION

This study essentially focused on the usage advantage of some neural networks in the prediction of COD removal performance of Classical-Fenton and Photo-Fenton Processes in laundry wastewater treatment. The results of RSM were also used in the comparison process. Four different experimental setups were designed for each of the Classical-Fenton and Photo-Fenton processes. As NN-based prediction models, the performances of SP-PSO, MLP-PSO, and MLP-LM were evaluated over the training, validity, and test sets. In addition, the prediction performance of RSM was discussed in comparison with the results produced by these three mod-

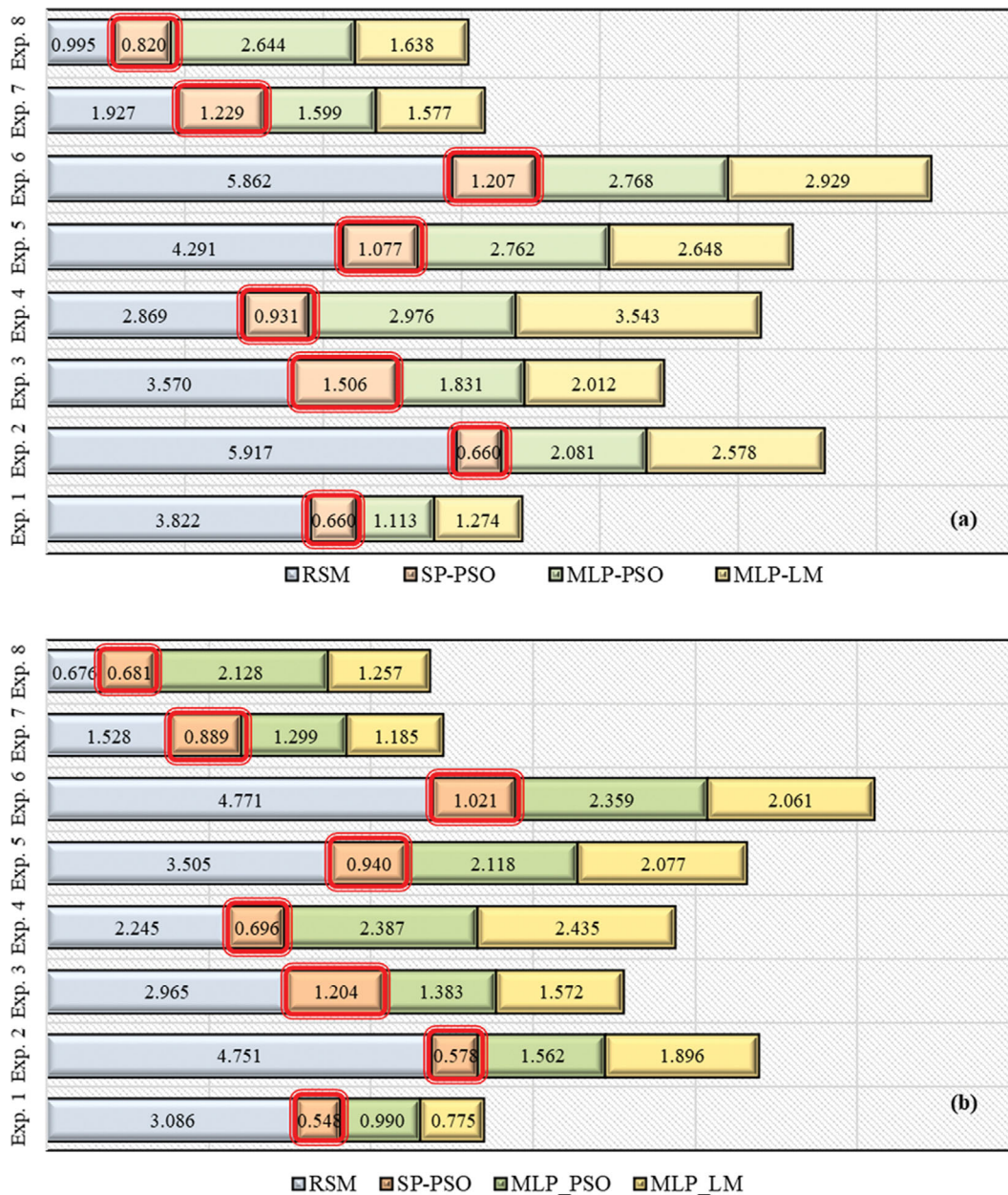


Fig. 6. Comparing the prediction models in terms of RMSE (a) and MAE(%) (b).

els for the whole data set. Another distinguishing aspect of this study is that the independent variables were optimized via GA for the best NN-based prediction model. When the results were evaluated as a whole, it was observed that NN-based models had superior predictive ability compared to RSM.

- Among NN-based models, SP-PSO produced the best predictive results in almost all cases.
- While SP-PSO produced predictions with RMSE values of around one in four out of eight experiments, these values were observed below one in the other four.
- According to the MAE criterion, which can be considered as a percentage error measure, SP-PSO produced predictions with errors of less than 1% in six out of eight experiments, while these errors were around 1% in the other two experiments.

- Considering the success rankings in terms of RMSE, while SP-PSO, for test and validation datasets, produced the best predictions in all cases except just one case, it produced the best predictions in all cases for training and all datasets.

- According to the success rankings in terms of MAE, while SP-PSO, for test and all datasets, produced the best predictions in all cases except just two cases for validation data sets. Moreover, for training data sets, it produced the best predictions in all cases.

- SP-PSO had satisfactory and competitive prediction ability even in the very few cases where it could not produce the best predictions.

The reasons behind the outstanding performance of SP-PSO can

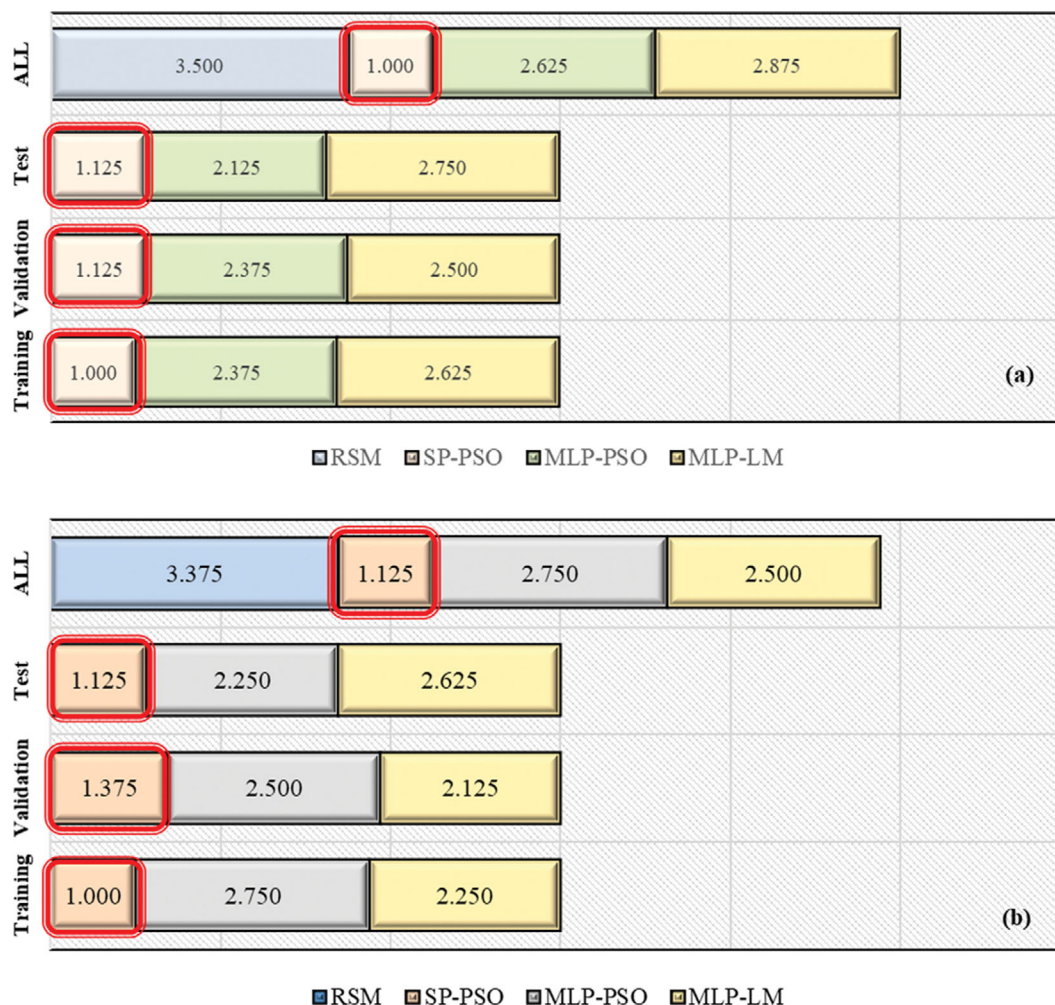


Fig. 7. Comparing all models in terms of RMSE (a) and MAE (b).

be summarized as follows:

- PSO used in the training process of the Sigma-Pi neural network is not stuck in local optimum traps, unlike LM which is a derivative-based training algorithm.
- Since the Sigma-Pi neural network uses a multiplicative aggregation function in its output layer's neuron, it is more flexible and successful in adaptation to a search space with a non-linear structure.

In addition to all these findings, the use of GA in optimizing the independent variables provided to get the optimal independent variables that will maximize the COD removal performance without the need for extra experiments. And when the optimum conditions were evaluated, it was seen that Photo-Fenton processes had a higher performance for laundry wastewater treatment than the Classical-Fenton process in each experiment. Furthermore, by using NN-based models as a prediction tool and determining optimal parameters with GA, both time and cost losses will be avoided and healthy and reliable results will be able to be obtained for possible experiments.

In future studies, it may be discussed to create hybrid models in which the models containing statistical approaches and the models based on NN are used together and to evaluate their performance.

#### AUTHORS' CONTRIBUTIONS

**Hüseyin Cüce:** Organized and Performed the experiments, Investigation, Reviewing. **Fulya Aydın Temel:** Data curation, Writing-Original draft preparation, Visualization, Investigation, Reviewing and Editing. **Özge Cagcag Yolcu:** Software, Validation, Writing-Original draft preparation, Investigation, Reviewing and Editing.

#### COMPETING INTERESTS

The authors declare that they have no competing interests.

#### REFERENCES

1. UNESCO, The United Nations World Water Development Report, 2003, pp. 92-3-103881-8.
2. B. Jefferson, A. Laine, S. Parsons, T. Stephenson and S. Judd, *Urban Water*, **1**(4), 285 (2000).
3. E. Friedler and M. Hadari, *Desalination*, **190**(1-3), 221 (2006).
4. E. L. Terechova, G. Zhang, J. Chen, N. A. Sosnina and F. Yang, *J. Environ. Chem. Eng.*, **2**(4), 2111 (2014).

5. A. K. Mostafazadeh, A. T. Benguit, A. Carabin, P. Drogui and E. Brien, *J. Water Process Eng.*, **28**, 277 (2019).
6. V. V. Patil, P. R. Gogate, A. P. Bhat and P. K. Ghosh, *Sep. Purif. Technol.*, **239**, 116594 (2020).
7. I. Ciabattia, F. Cesaro, L. Faralli, E. Fatarella and F. Tognotti, *Desalination*, **245**(1-3), 451 (2009).
8. A. G. L. Moura, V. B. Centurion, D. Y. Okada, F. Motteran, T. P. Delforno, V. M. Oliveira and M. B. A. Varesche, *J. Environ. Manage.*, **251**, 109495 (2019).
9. A. Dimoglo, P. Sevim-Elibol, Ö. Dinç, K. Gökmen and H. Erdoğan, *J. Water Process Eng.*, **31**, 100877 (2019).
10. J. Ge, J. Qu, P. Lei and H. Liu, *Sep. Purif. Technol.*, **36**(1), 33 (2004).
11. B. G. Chooobar, M. A. A. Shahmirzadi, A. Kargari and M. Manouchehri, *J. Environ. Chem. Eng.*, **7**(2), 103030 (2019).
12. A. K. Huang, M. T. Veit, P. T. Juchen, G. D. C. Gonçalves, S. M. Palácio and C. D. O. Cardoso, *J. Environ. Chem. Eng.*, **7**(4), 103226 (2019).
13. A. Sumisha, G. Arthanareeswaran, Y. L. Thuyavan, A. F. Ismail and S. Chakraborty, *Ecotoxicol. Environ. Saf.*, **121**(2004), 174 (2015).
14. O. Turkay, S. Barişçi and M. Sillanpää, *J. Environ. Chem. Eng.*, **5**(5), 4282 (2017).
15. T. H. Kim, C. Park, J. Yang and S. Kim, *J. Hazard. Mater.*, **112**(1-2), 95 (2004).
16. H. Li, Y. Li, L. Xiang, Q. Huang, J. Qiu, H. Zhang, M. V. Sivaiah, F. Baron, J. Barrault, S. Petit and S. Valange, *J. Hazard. Mater.*, **287**, 32 (2015).
17. N. C. Fernandes, L. B. Brito, G. G. Costa, S. F. Taveira, M. S. S. Cunha-Filho, G. A. R. Oliveira and R. N. Marreto, *Chem. Biol. Interact.*, **291**, 47 (2018).
18. N. Ertugay and F. N. Acar, *Arab. J. Chem.*, **10**, S1158 (2017).
19. J. M. Poyatos, M. M. Muñoz, M. C. Almecija, J. C. Torres, E. Honoria and F. Osorio, *Water. Air. Soil Pollut.*, **205**(1-4), 187 (2010).
20. F. Emami, A. R. Tehrani-Bagha, K. Gharanjig and F. M. Menger, *Desalination*, **257**(1-3), 124 (2010).
21. K. Paździór, L. Bilińska and S. Ledakowicz, *Chem. Eng. J.*, **376**, 120597 (2019).
22. U. Yolcu, Y. Jin and E. Egrioglu, 2016 IEEE Symp. Ser. Comput. Intell. SSCI 2016 (2017).
23. U. Yolcu, E. Egrioglu, E. Bas, O. C. Yolcu and A. Z. Dalar, *J. Exp. Theor. Artif. Intell.*, **33**(3), 383 (2021).
24. O. Cagcağ Yolcu, E. Bas, E. Egrioglu and U. Yolcu, *Neural Process. Lett.*, **47**(3), 1133 (2018).
25. E. Baştürk and A. Alver, *J. Environ. Manage.*, **248**, 109300 (2019).
26. E. S. Elmolla, M. Chaudhuri and M. M. Eltoukhy, *J. Hazard. Mater.*, **179**(1-3), 127 (2010).
27. M. Radwan, M. G. Alalm and H. Eletriby, *J. Water Process Eng.*, **22**, 155 (2018).
28. M. R. Sabour and A. Amiri, *Waste Manag.*, **65**, 54 (2017).
29. S. Talwar, A. K. Verma and V. K. Sangal, *J. Environ. Manage.*, **250**, 109428 (2019).
30. A. Tolba, M. G. Alalm, M. Elsamadony, A. Mostafa, H. Afify and D. D. Dionysiou, *Process Saf. Environ. Prot.*, **128**, 273 (2019).
31. A. M. Gholizadeh, M. Zarei, M. Ebratkhahan and A. Hasanzadeh, *J. Environ. Chem. Eng.*, **9**(1), 104999 (2021).
32. N. Jaafarzadeh, M. Ahmadi, H. Amiri, M. H. Yassin and S. S. Martinez, *J. Taiwan Inst. Chem. Eng.*, **43**(6), 873 (2012).
33. R. B. Baird, A. D. Eaton and E. W. Rice, *Standard methods for the examination of water and wastewater*, 23<sup>rd</sup> Ed., American public health association, Washington, DC (2017).
34. P. J. Werbos, *The roots of backpropagation*, John Wiley & Sons, New York (1974).
35. Y. Shin and J. Gosh, *IJCNN-91-Seattle International Joint Conference on Neural Networks*, **1**, 13 (1991).
36. J. Kennedy and R. Eberhart, *Proceedings of IEEE international conference on neural networks*, Piscataway, NJ: IEEE Service Center, Perth, Australia, 1942 (1995).
37. J. H. Holland, *Adaptation in natural and artificial systems: An introductory analysis with applications to biology, control, and artificial intelligence*, MIT Press, London, England (1992).
38. D. E. Goldberg, *Genetic algorithms in search, optimization and machine learning 13<sup>th</sup> Ed. Edition*, Addison-Wesley Publishing Company, Boston, United States (1989).